International Journal for Parasitology (2016), 46(8): 507-517. doi:10.1016/j.ijpara.2016.03.007

RNA-seq analysis of early enteromyxosis in turbot (*Scophthalmus maximus*): new insights into parasite invasion and immune evasion strategies

Paolo Ronza [a,1], Diego Robledo [b,1], Roberto Bermúdez [c], Ana Paula Losada [a], Belén G. Pardo [d], Ariadna Sitjà-Bobadilla [e], María Isabel Quiroga [a,*], Paulino Martínez [d]

[a]*Departamento de Ciencias Clínicas Veterinarias, Facultad de Veterinaria, Universidade de Santiago de Compostela, 27002 Lugo, Spain*

[b]*Departamento de Genética, Facultad de Biología (CIBUS), Universidade de Santiago de Compostela, 15782 Santiago de Compostela, Spain*

[c]*Departamento de Anatomía y Producción Animal, Facultad de Veterinaria, Universidade de Santiago de Compostela, 27002 Lugo, Spain*

[d]*Departamento de Genética, Facultad de Veterinaria, Universidade de Santiago de Compostela, 27002 Lugo, Spain*

[e]*Instituto de Acuicultura Torre de la Sal (IATS-CSIC), 12595 Ribera de Cabanes, Castellón, Spain*

[1]Authors contributed equally to this article.

*****Corresponding author: María Isabel Quiroga, Departamento de Ciencias Clínicas Veterinarias, Facultad de Veterinaria, Universidade de Santiago de Compostela, 27002 Lugo, Spain.
Tel.: +34 982822304; fax: +34 982252195.

E-mail address: misabel.quiroga@usc.es

Abstract

Enteromyxum scophthalmi, an intestinal myxozoan parasite, is the causative agent of a threatening disease for turbot (*Scophthalmus maximus*, L.) aquaculture. The colonization of the digestive tract by this parasite leads to a cachectic syndrome associated with high morbidity and mortality rates. This myxosporidiosis has a long pre-patent period and the first detectable clinical and histopathological changes are subtle. The pathogenic mechanisms acting in the early stages of infection are still far from being fully understood. Further information on the host-parasite interaction is needed to assist in finding efficient preventive and therapeutic measures. Here, a RNA-seq-based transcriptome analysis of head kidney, spleen and pyloric caeca from experimentally-infected and control turbot was performed. Only infected fish with early signs of infection, determined by histopathology and immunohistochemical detection of *E. scophthalmi*, were selected. The RNA-seq analysis revealed, as expected, less intense transcriptomic changes than those previously found during later stages of the disease. Several genes involved in IFN-related pathways were up-regulated in the three organs, suggesting that the IFN-mediated immune response plays a main role in this phase of the disease. Interestingly, an opposite expression pattern had been found in a previous study on severely infected turbot. In addition, possible strategies for immune system evasion were suggested by the down-regulation of different genes encoding complement components and acute phase proteins. At the site of infection (pyloric caeca), modulation of genes related to different structural proteins was detected and the expression profile indicated the inhibition of cell proliferation and differentiation. These transcriptomic changes provide indications regarding the mechanisms of parasite attachment to and invasion of the host. The current results contribute to a better knowledge of the events that characterize the early stages of turbot enteromyxosis and provide valuable information to identify molecular markers for early detection and control of this important parasitosis.

Keywords: RNA-seq, Transcriptome, Turbot, *Enteromyxum scophthalmi,* Myxozoa, Pathogenesis

1. Introduction

Turbot (*Scophthalmus maximus*, L.) is a valuable cultured marine flatfish, whose production in 2013 accounted for over 77,000 tons, with China (67,000 tons in 2013) and the European Union (7,700 tons in 2013, 11,000 in 2014) as the main producers (APROMAR, 2015). Enteromyxosis caused by *Enteromyxum scophthalmi* (Myxozoa) is a serious threat for turbot aquaculture, currently without effective therapeutic measures (Sitjà-Bobadilla and Palenzuela, 2012). The target site of this myxozoan parasite is the gastrointestinal tract, where it proliferates and spreads from the anterior intestine and pyloric caeca to other gut regions (Redondo et al., 2004). The infection leads to severe catarrhal gastroenteritis associated with a cachectic syndrome, with reduction of growth performance and high mortality rates (Bermúdez et al., 2010; Sitjà-Bobadilla and Palenzuela, 2012). Under culture conditions, the trophozoites are transmitted directly from fish to fish, which leads to a rapid spread of disease in infected tanks and facilities (Redondo et al., 2002; Quiroga et al., 2006; Sitjà-Bobadilla and Palenzuela, 2012). However, the disease shows a long pre-patent period, with the parasite detectable in the digestive tract by histology only after several weeks in natural infections (Redondo et al., 2004; Quiroga et al., 2006). In experimental infections by effluent transmission or cohabitation, the parasite is first observed at approximately 20 days post-exposure, and at approximately 8 days after experimental per os transmission (Redondo et al., 2004; Bermúdez et al., 2006; Sitjà-Bobadilla et al., 2006; Losada et al., 2014a). Experimental infection by the oral route results in a very high and quick prevalence of infection and homogeneous lesions in recipient fish. In addition, the ingestion of trophozoites released from infected fish is thought to be the main infection route occurring in the fish farm (Redondo et al., 2002, 2004). In the early stages of infection there are no external clinical signs, histological lesions are very subtle, and the parasite is difficult to detect in conventional histological sections of the digestive tract (Quiroga et al., 2006; Bermúdez et al., 2010). In vitro, *E. scophthalmi* is able to penetrate the intestinal epithelium from the lumen as well as via the basement membrane, and the report of parasitic stages in blood smears

suggests the existence of a haematic route of spread (Redondo et al., 2003, 2004; Redondo and Álvarez-Pellitero, 2010). However, a detailed understanding of entry routes and epithelial invasion strategies is lacking. We are still far from a full knowledge of the host-parasite interaction and further investigation is needed to clarify the pathogenetic mechanisms of enteromyxosis (Sitjà-Bobadilla and Palenzuela, 2012; Robledo et al., 2014), especially those acting during early stages of infection.

Whole-transcriptome analysis using RNA-seq is a suitable approach for the identification of the genes and pathways involved in host-pathogen interactions, and it is acquiring a key role in the understanding of the pathogenesis of human and veterinary diseases (Costa et al., 2013; Qian et al., 2014; Li et al., 2015). This is an essential starting point for the development of control measures, therapeutic options and genetic breeding programs. An RNA-seq analysis of turbot experimentally infected by the oral route was previously addressed, investigating the advanced stages of the disease by studying specimens at 42 days post-inoculation. That work enabled a better understanding of the genetic basis of the clinical signs and lesions which characterize the infection (Robledo et al., 2014). In this study, using a similar methodological approach, we performed a transcriptomic analysis of turbot showing very early signs of infection aimed at contributing to the current understanding of incipient enteromyxosis.

2. Materials and methods

2.1. Experimental design

The experimental setup and sampling were as previously described (Robledo et al., 2014). Briefly, infection was achieved by the oral route (Redondo et al., 2002) and tissue samples were collected in Bouin's fluid and RNAlater (Qiagen, Germany) for histological techniques and RNA-seq, respectively. A histological evaluation was performed, and infected turbot were classified into

three groups (slightly, moderately and severely infected) according to the histopathological grading described by Bermúdez et al. (2010). For RNA-seq analysis, spleen, head kidney and pyloric caeca from three control (CTRL) and three *E. scophthalmi*-infected (recipient, RCPT) fish at 24 days post-inoculation were used. The three RCPT fish were selected by histology among those graded as slightly infected and numbered (infected turbot 1, 2 and 3). RNA aliquots from the samples of RCPT fish were sequenced individually, while samples from CTRL fish were pooled by organ, resulting in three RCPT and one CTRL sample per organ.

2.2. Immunohistochemistry

Immunohistochemical detection of *E. scophthalmi* was performed on sections from different regions of the digestive tract (oesophagus, stomach, pyloric caeca, anterior, middle and posterior intestine) to confirm the presence of the parasite. Thin sections (3 μm) were placed on slides treated with silane to improve section adherence and dried overnight at 37 ºC. After deparaffination (two 5 min washes in xylene) and rehydration (graded alcohol series), the endogenous peroxidase activity was inhibited by incubating the slides with peroxidase-blocking solution (Dako, Denmark) for 40 min. A 2 h incubation at room temperature was performed with a polyclonal antibody against *E. scophthalmi* (Estensoro et al., 2014) (diluted 1: 50,000). The secondary antibody conjugated with peroxidase was the anti-rabbit EnVision+ System Labelled Polymer-HRP (Dako) for 30 min, followed by development with diaminobenzidine (Dako). All incubations were performed in humid chambers and three 5 min washes with 0.01 M PBS were carried out between all subsequent steps. Sections of severely infected turbot were used as positive controls. In the sections included as negative controls, the primary antibody was replaced by antibody diluents.

2.3. RNA-seq and differential expression analysis

Some of the procedures and methodologies employed were described previously (Robledo et al., 2014). Briefly, RNA extraction was performed using the RNeasy mini kit (Qiagen, Germany) with DNase treatment and RNA quality and quantity were evaluated in a Bioanalyzer (Bonsai Technologies, Spain) and in a NanoDrop® ND-1000 spectrophotometer (NanoDrop® Technologies Inc., Delaware, US), respectively. The samples were barcoded and prepared for sequencing by the Wellcome Trust Centre for Human Genetics (Oxford, UK) and sequenced on an Illumina HiSeq 2000 as 100 bp paired-end reads. All the data files have been deposited in the National Center for Biotechnology Information (NCBI) Short Read Archive (SRA) database under the project ID PRJNA300347; as well the generated transcriptome sequences and their annotation have been deposited in Mendeley Data (https://data.mendeley.com/) and can be accessed using doi: 10.17632/3vhc8py3cv.2. Quality filtering and removal of residual adaptor sequences was conducted using Trimmomatic v.0.32 (Bolger et al., 2014). The recently assembled turbot genome (Figueras et al., 2016) was used as a reference for read mapping. Filtered reads were mapped to the genome using Tophat2 v.2.0.11 (Kim et al., 2013) which leverages the short read aligner Bowtie2 v.2.2.3 (Langmead and Salzberg, 2012) with a maximum intron length of 20 kb. HTSeq-count (http://www-huber.embl.de/users/anders/HTSeq/doc/overview.html) was used to extract the raw reads from the mapping files and differentially expressed genes were obtained using EdgeR (Robinson and Oshlack, 2010) with a False Discovery Rate (FDR) corrected *P* value of 0.05. The differentially expressed (DE) genes were identified and annotated using Blast2GO v.2.7.0 (Conesa et al., 2005) with an E-value cutoff of E^{-6}. Enriched Gene Ontology (GO) terms for each organ were identified by comparing the DE genes against the full transcriptome using Blast2GO Fisher's exact test ($P < 0.05$, FDR corrected). Furthermore, in this study, Kyoto Encyclopedia of Genes and Genomes (KEGG, Kanehisa et al., 2016)) enrichment was assessed using KOBAS 2.0 (Wu et al., 2006) ($P < 0.05$, FDR corrected) with the draft turbot genome annotation as background. Those reads from pyloric caeca samples which did not align against the genome, both from turbot of this study (at 24 days post-inoculation) and from a previous study with parasitized turbot at 42 days

post-inoculation (Robledo et al. 2014), were extracted and de novo transcriptome assembly was carried out using ABySS (version 1.3.7; Simpson et al., 2009) with a 64 k-mer size, scaffolding and contig options on, and remaining parameters set to default values. Expression values were individually estimated for each pyloric caeca sample by counting reads for each transcript after aligning the genome-unaligned reads of the sample against the reconstructed de novo transcriptome using RSEM v.1.2.17 (Li and Dewey, 2011). Differential expression between infected and control groups was estimated using EdgeR (FDR corrected P value < 0.05; Robinson and Oshlack, 2010).

3. Results and discussion

3.1. Histopathology revealed minor tissue alterations and the presence of E. scophthalmi

The histological evaluation of RCPT turbot revealed minor alterations at an intestinal level. Slight inflammatory infiltrates, mostly composed of mononuclear cells, were occasionally detected in the lamina propria-submucosa or at the base of the epithelial lining of pyloric caeca and anterior intestine (Fig. 1A, B, D). In these areas, basophilic structures consistent with early stages of the parasite were observed (Fig. 1A, B). The specimen labelled as "infected turbot 2" also presented some trophozoites in the hindgut, and was the only fish which sporadically showed more advanced developmental stages of *E. scophthalmi*, stages 2 or 3 according to Redondo et al. (2004) (Figs. 1D, E). The histological features of the three RCPT fish were in accordance with the "slight infection" degree described by Bermúdez et al. (2010). No significant changes were detected in the remaining examined organs, nor in CTRL fish. The presence of parasitic stages was then confirmed by immunohistochemistry (Fig. 1C, F), supporting the histological observations.

3.2. Pyloric caeca showed higher percentages of unaligned reads

A total of ~170 million 100 bp pair-end reads were sequenced, the same amount as in the previous work with severely infected turbot, accounting on average for 13.3 million reads post-filtering per sample, slightly below the 15 million reads per sample formerly obtained (Robledo et al., 2014). A total of 138 million (86.5%) of the filtered reads (~160 million) were mapped to the turbot genome. A notable difference was found between this and the previous study when comparing the result of the alignments for pyloric caeca. In slightly infected turbot, 90% of the trimmed reads aligned to the genome, while in severely infected turbot only 65% aligned (Robledo et al., 2014). The unaligned reads of both 24 and 42 days post-inoculation samples from pyloric caeca were used to reconstruct a de novo transcriptome (a brief comparison between genome-guided and de novo assemblies is shown in Table 1), and differential expression analysis between infected and control samples was carried out. No sequences annotated to *Enteromyxum* spp. were detected among DE genes at 24 days post-inoculation, but six transcripts, annotated as *E. scophthalmi* 18S subunit ribosomal gene, and two more as *Enteromyxum leei* 28s subunit ribosomal gene, were found DE at 42 days post-inoculation. The fact that no DE *Enteromyxum* sequences were found during early stages of the disease suggests that the concentration of the parasite in pyloric caeca at that stage is low. On the other hand, another 422 up-regulated sequences were found in pyloric caeca samples at 42 days post-inoculation, showing zero or one read in the control, and annotated to invertebrate, plant, bacteria or fungi sequences (Supplementary Table S1). Some of these sequences may correspond to new *Enteromyxum* sequences and constitute a resource for exploration of host-parasite interactions in future studies, while others, especially those annotated to bacteria, might reflect gut microbiota alterations caused by the disease.

3.3. Transcriptomic changes are subtle at early stages of infection

The aligned reads resulted in a total of 56,321 transcripts from 36,356 genes. Samples were hierarchically clustered for each organ according to their transcript expression (Fig. 2). Samples

corresponding to the infected turbot 2 always clustered closest to the control samples, suggesting a less intense response to infection. This is a remarkable result considering that this was the specimen presenting more advanced stages of *E. scophthalmi* and more widespread and might suggest silencing of the host response during some stages of the infection and/or an interindividual response variation. On the other hand, infected turbot 1 and 3 constituted a different cluster only in pyloric caeca, likely related to the stronger effect of the infection in this organ.

A total of 287, 211 and 187 DE genes were detected in head kidney, spleen and pyloric caeca, highlighting the huge transcriptomic changes between the early and the advanced stage of the disease, where the numbers were 1,316, 1,377 and 3,022, respectively (Robledo et al., 2014). As previously described (Robledo et al., 2014), relevant DE genes were grouped in five key broad functional categories: immune and defence response, apoptosis and cell proliferation, cytoskeleton and extracellular matrix, iron metabolism and erythropoiesis, and metabolism and digestive function. Yet, in this study, DE genes related to cell differentiation were included in the category "apoptosis and cell proliferation", being renamed as "apoptosis, cell proliferation and differentiation" (Supplementary Tables S2 - S4). Heatmaps of selected DE genes (Fig. 3), over-represented GO terms (Fig. 4) and Venn diagrams comparing the total number of DE genes in the early and advanced stages (24 and 42 days post-inoculation, Fig. 5 and Supplementary Table S5 – S7) are presented.

3.4. Immune and defence response: possible strategies for immune evasion and activation of interferon-related pathways

Some mechanisms of innate immunity were active during both early and late stages of the disease (Robledo et al., 2014), such as the up-regulation in kidney and spleen of *ALOXE3* (full gene names are shown in Supplementary Tables S2 - S4), acting on the metabolism of leukotrienes,

and *IL4I,* which participates in antigen processing. Also, *CD209*, a C-type lectin considered a marker of antigen-presenting cells, was up-regulated in pyloric caeca as in the previous study, adding new evidence about the role of this molecule in recognizing *E. scophthalmi*. In spleen, up-regulation of genes related to endothelin, a vasoconstrictor peptide and chemoattractant of macrophages, was also found in both studies. In early enteromyxosis, other up-regulated genes acting in innate immunity were *C1QTNF9* and *GF1B* in spleen and pyloric caeca (Supplementary Tables S3, S4), involved in inflammatory response, and *CCL19* in head kidney (Supplementary Tables S2), a chemokine with chemotactic properties on lymphocytes and dendritic cells. On the other hand, up-regulated genes associated with inhibition of the immune response were also detected, such as *ZNFX1* in kidney and pyloric caeca, the transcription factor *FOXJ1* in pyloric caeca and spleen, and *FOXJ1B* only in pyloric caeca. In the latter organ, these genes were related to the over-represented GO terms associated with negative regulation of immune-related processes (Fig. 4).

Some complement-related genes were down-regulated in the three organs. The most remarkable result was detected in spleen, where the KEGG pathway "complement and coagulation cascades" was enriched due to the down-regulation of several genes that constitute it (Supplementary Fig. S1). Many products of these genes are considered acute phase proteins (APP), such as the same complement components and different antiproteases. Also, other APP genes such as haptoglobin, transferrin and ceruloplasmin, related to iron metabolism and antioxidant capacity, were down-regulated in spleen. The acute phase response is an evolutionarily conserved immune mechanism activated in teleosts by several infective agents including parasites (Bayne and Gerwick, 2001; Gerwick et al., 2002; Peatman et al., 2007; Khoo et al., 2012; Kovacevic et al., 2015). By contrast, in the current parasite model, the opposite pattern was detected. This may reflect a parasite-induced down-regulation as a strategy for immune system evasion or may be a temporary exhaustion of this pathway following a previous activation. The first hypothesis would agree with

the pathogens targeting the complement system and host antiproteases as immune evasion strategies (Armstrong, 2006; Zipfel et al., 2007), as well as with mechanisms for iron acquisition from host cells (Ben-Othman et al., 2014; Leon-Sicairos et al., 2015). The second hypothesis would be in accordance with previous observations in turbot exposed to *E. scophthalmi* by cohabitation (a slower infection model), where serum complement activity by the alternative pathway was slightly increased in infected fish at 20 days post-exposure but later (40 days post-exposure) decreased in comparison with naïve fish (Sitjà-Bobadilla et al., 2006). Since the liver is the main producer of complement components and APP, a time series study of the hepatic gene expression profile would help to clarify this response during enteromyxosis.

Another result that strongly characterized this functional category was the up-regulation of several genes related to the IFN-mediated immune response. The *PML* gene, which positively regulates the type I IFN response by promoting transcription of IFN-stimulated genes (ISGs) (Kim and Ahn, 2015), was up-regulated in the three organs. Head kidney showed the highest number of DE genes related to IFN signalling, with an increased expression of IFN-γ, and sharing up-regulation of IFN-induced Mx protein, *HERC4/5* and *IFIT1* with pyloric caeca and of *IFI44* and IFN-inducible protein gig2 with spleen. All in all, these results point towards a response mediated by both type I and II IFNs, as observed in early stages of several mammalian protozoan infections (Beiting, 2014). Also, the IFN-mediated immune response was shown to play a major role in teleosts parasitized by amoebae and myxozoan parasites, with implications in fish resistance or susceptibility to the disease (Young et al., 2008; Davey et al., 2011; Bjork et al., 2014). During advanced stages of turbot enteromyxosis, IFN-related genes were markedly down-regulated in the same organs, possibly indicating an association between the exhaustion of the IFN-mediated response and the high susceptibility of turbot to enteromyxosis (Robledo et al., 2014). On the other hand, this opposite pattern may also suggest that the immune response to *E. scophthalmi* is elicited

differently during the two stages of infection, perhaps depending on a change in the localization of the parasite during the infection.

In this sense, the up-regulation of *STING* (also called *MITA*), *DHX58* and *TRIM25* observed in head kidney and *MFN1* in pyloric caeca suggests activation of the RIG-I-like receptors (RLRs) pathway. This pathway triggers the innate immune response against intracellular pathogens, promoting the production of type I IFNs, ISGs and proinflammatory cytokines (Dixit and Kagan, 2013). RLR activation involves the participation of mitochondria, signalled through the mitochondrial antiviral signalling protein (MAVS, also called IPS1) (Castanier et al., 2010; Koshiba, 2013). *MFN1* mediates mitochondria fusion and encodes for a protein associated with MAVS on the outer membrane of mitochondria, both being necessary for signal transduction in the RLR pathway through the regulation of mitochondria dynamics (Castanier et al., 2010; Onoguchi et al., 2010). This pathway is mainly known for viral recognition, but some evidence is emerging for type I IFN production promoted by parasite-activated RLRs (Melo et al., 2013; Beiting, 2014). Little is known about the pre-patent phase of enteromyxosis, but intracellular parasitic stages have been described sporadically (Redondo et al., 2003, 2004; Quiroga et al., 2006), so it may be hypothesized that an intracellular phase occurs during *E. scophthalmi* infection where the parasite is recognized by RLRs. Head kidney also showed increased expression of *TRIM21*, described as an intracellular antibody receptor and regulator of IFN pathways acting in viral infections (McEwan et al., 2013; Vaysburd et al., 2013; Manocha et al., 2014), and of *SOCS1*, which plays an evolutionarily conserved inhibitory role in the IFN signalling pathway (Nie et al., 2014). The number of DE genes classically involved in antiviral defence showed by kidney is reflected by the corresponding enriched GO term found, together with other immune-related categories (Fig. 4). Both types of IFNs are also related to antigen presentation to cytotoxic cells via the major histocompatibility complex class I (MHC-I) in teleosts (Zou and Secombes, 2011). In head kidney, we found up-regulation of *HSP70* and *HSP90*, which participate in antigen presentation via the

MHC-I pathway, as do calreticulin and the MHC-I genes, whose expression was significantly increased in one of the three infected fish (data not shown). The activation of natural killer (NK) and cytotoxic T-cells was reflected by the up-regulation of *GZMA* in kidney and spleen, and *PRF1* in kidney, both codifying for cytolytic proteins found in granules of these cell types. MHC-I and T-cells-related genes also showed an opposite expression pattern in the lymphohaematopoietic organs of turbot with advanced enteromyxosis (Robledo et al., 2014).

In pyloric caeca, two up-regulated genes related to T-cells were detected, *LRRC32*, a regulatory T (T-reg) specific receptor (Tran et al., 2009), and *NFIL3*, a transcription factor with several important roles in the immune response, such NK cell function development, IL-3 transcription in T-cells and regulation of the Th2 cell response (Zhang et al., 1995; Kashiwada et al., 2011). On the other hand, the gene for the T-cell surface antigen CD2 was down-regulated in kidney and pyloric caeca. This molecule is present on T and NK cells, where it plays a role in cell adhesion and acts as a co-stimulatory molecule for these cells. Decreased expression of *CD2* has been found to be associated with infection by *Leishmania donovani* in human, causing impaired $CD4^+$ T-cell function and protective IFN-γ production (Bimal et al., 2008).

With regard to adaptive immunity, *RAG1*, a key gene for rearrangement and recombination of immunoglobulin and T-cell receptor molecules during the VDJ recombination process, was up-regulated in spleen. Nonetheless, little evidence was found for the activation of B cells, in accordance with previous observations of a delayed humoral response (Bermúdez et al., 2006; Sitjà-Bobadilla et al., 2006). Only pyloric caeca showed up-regulation of *PAX5*, a transcription factor with a major role in B cells differentiation, and of the immunoglobulin-related gene Ig heavy chain Mem5. Other interesting up-regulated genes in pyloric caeca, the target organ of the parasite, were *RAC1*, a member of the small GTPase family, and *ACK1*, a downstream effector of another member of this family, *CDC42*. These genes act in the c-Jun N-terminal protein kinases (JNK) pathway and are involved in actin cytoskeleton remodelling induced by extracellular signals (Chen et al., 2004).

They have been implicated in host cell invasion by different pathogens including protozoan parasites (Gruenheid and Finlay, 2003; Chen et al., 2004; Lodge and Descoteaux, 2006).

3.5. Cytoskeleton and extracellular matrix: unravelling mechanisms of parasite attachment and invasion

Different genes encoding for components of the intracellular cytoskeleton (e.g. *FLNC*, *SYNM* and *SYNPO2*) were down-regulated in pyloric caeca, suggesting parasite-induced cytoskeleton remodelling of intestinal cells. Host cytoskeleton is a recognized early target of several pathogens that infect epithelia for invasion of the host (Gruenheid and Finlay, 2003; Xu et al., 2008; Radhakrishnan and Splitter, 2012), a mechanism also observed in teleost skin, gill and digestive tract (Li et al., 2012, 2013; Sun et al., 2012). Another interesting adjustment in pyloric caeca was the up-regulation of genes encoding for extracellular matrix (ECM) components such as *COL1A1*, *TNN* and *FREM1*. The expression changes in genes related to ECM proteins may be difficult to interpret because they might reflect either an early attempt at tissue repair by the host or the pathogen manipulation and infection (Li et al., 2013). In fact, ECM proteins are often targeted by many invasive pathogens, including parasites, for adhesion to and invasion of the host (Mittal et al., 2008; Nde et al., 2012; Singh et al., 2012). Interestingly, *FREM1* has been recently postulated as a novel candidate gene involved in human immunodeficiency virus (HIV) infection (Luo et al., 2012). *Enteromyxum scophthalmi* is capable of attaching to and penetrating the intestinal epithelium, both from the surface and the basal part, as shown by in vitro studies with intestinal explants (Redondo et al., 2004; Redondo and Álvarez-Pellitero, 2010). In addition, in different experimental infections it was observed that a longer time is needed to detect the parasite in intestinal histological sections than in blood smears, blood being a hypothesized dispersion route (Redondo et al., 2003, 2004). Hence, the possibility of epithelial invasion through the lamina propria-submucosa, involving an interaction with ECM proteins, cannot be ruled out. Finally, a group of up-regulated DE genes in

this location were related to cell-cell junctions, in particular three genes encoding for claudins (*CLDN10*, *CLDN14* and *CLDN18*), tight junction proteins, and for the adhesion protein *CDH26*. These results are in accordance with the increasing expression trend found by real-time PCR for E-cadherin (CDH1) in turbot with incipient infection (unpublished data). The junctional complexes are essential to maintain the homeostasis of the intestinal barrier (Suzuki, 2013; Peterson and Artis, 2014) and this expression profile may be indicative of early repair mechanisms in response to the parasite invasion of the lining epithelium. In advanced infection, it is plausible that the extension of lesions, the severe inflammation and the prolonged fasting suffered by fish (Bermúdez et al., 2010; Robledo et al., 2014) hinder an efficient activation and functioning of tissue repair at an intestinal level.

3.6. Apoptosis, cell proliferation and differentiation: *effects of E. scophthalmi on intestinal renewal*

In addition to epithelial integrity, the constant renewal of the epithelium is a main defence mechanism of the intestine against pathogens, and consequently a target for microbial circumvention strategies (Kim et al., 2010). Accelerating the epithelial turnover has been described as a host mechanism for parasite expulsion (Cliffe et al., 2005; Cortes et al., 2015), but several mucosal pathogens can put in place stratagems to prevent their removal and successfully colonize the lining epithelium (Iwai et al., 2007; Mimuro et al., 2007). In pyloric caeca of *E. scophthalmi*-infected fish, there was a remarkable down-regulation of numerous genes related to cell proliferation (e.g. *CCNB1*, *TPX2* and *CDC14A*) and differentiation (e.g. *HOXA9 HOXA10*, *VSIG1*). Furthermore, *APC* and *TLX1*, which by contrast act as repressors of cell proliferation and differentiation, showed an increased expression. Also *CASP3*, involved in apoptosis, was down-regulated, unlike that observed in severely-infected turbot, which presented up-regulation of this and other pro-apoptotic genes (Robledo et al., 2014). A biphasic modulation of apoptotic pathways, consisting of early inhibition and late moderate promotion, was documented in human infection by

the intestinal parasite *Cryptosporidium parvum* (Liu et al., 2009). All in all, DE genes of this functional category suggest that inhibitory mechanisms of epithelial renewal occur during incipient enteromyxosis, which may facilitate the parasite's entrance and colonization of the digestive tract. At later infection stages, the pathological changes observed in the intestinal epithelium, including the increased apoptotic rate and enterocyte detachment, may be invoked by the exacerbated local immune response (Bermúdez et al., 2010; Losada et al., 2012, 2014a; Robledo et al., 2014) and/or induced by the parasite as a spreading strategy (Bermúdez et al., 2010). The only up-regulated gene promoting cell proliferation was *CTGF*, a major connective tissue mitoattractant also involved in ECM secretion, a finding in accordance with the aforementioned up-regulation of different ECM-related genes.

3.7. Iron metabolism and erythropoiesis

Several genes related to haemoglobin (*HBB2* and *HBAD*), iron homeostasis and heme biosynthesis (*FAM123B*; *SLC25A37* and *ALAS2*), and erythrocyte maturation and differentiation (*GATA2* and *TAL1*) showed an increased expression in pyloric caeca. Genes related to erythrocyte structural (*DMTN*, *ANK1* and *RHAG*) and enzymatic (*CA*) components were also up-regulated. These findings point towards an increased presence of red blood cells in the intestine of infected turbot, consistent with hyperaemia. Hyperaemia is one of the first vascular changes which occur after an inflammatory stimulus (McGavin and Zachary, 2006), a scenario consistent with early infection of the digestive tract. On the other hand, a gene related to hepcidin (*HEP-2*), a main regulator of iron metabolism, was down-regulated. In turbot, the existence of two hepcidin genes has been reported (*HEP-1* and *HEP-2*), both showing antimicrobial properties and modulated expression in response to bacterial and viral challenges (Pereiro et al., 2012; Zhang et al., 2014). Nevertheless, a major role for *HEP-1* in body iron homeostasis has been previously suggested, given that *HEP-2* expression did not change in liver in response to iron overload (Pereiro et al.,

2012). In our case, the down-regulation of *HEP-2* in pyloric caeca may be related to the requirement of iron for heme biosynthesis, a hypothesis also supported by the contemporary up-regulation of *FAM123B*. The product of this gene is known as erythroferrone, an iron-regulatory hormone with a potent suppressor action on hepcidin mRNA expression in mice (Kautz et al., 2014). Under the hypotheses of a main role for *HEP-2* in innate immune response and considering the expression profile of APP-related genes in the spleen, its down-regulation should also be interpreted in the context of a global modulation of the immune response. Further research is needed to clarify the role of APP and iron metabolism regulation during infection by *E. scophthalmi*.

3.8. Metabolism and digestive function: diminished feeding activity

DE genes involved in digestive function were mostly down-regulated, including *VIP*, *NPY2R* and *APOA4*. The only exception was the up-regulation of *GCG2*, a paralog of the glucagon gene, which promotes hydrolysis of glycogen and lipids, thus increasing blood sugar levels (Moon, 1998). In previous immunohistochemical studies on the digestive tract of turbot with advanced enteromyxosis, both VIP- and glucagon-immunoreactive cells showed decreases (Bermúdez et al., 2007; Losada et al., 2014b). Also, *APOA4*, involved in lipids metabolism, was down-regulated in the pyloric caeca of severely infected turbot analyzed by RNA-Seq (Robledo et al., 2014). The down-regulation of a receptor of neuropeptide Y (*NPY2R*), a main regulator of appetite which stimulates food intake (Zhou et al., 2013), may indicate that the changes leading to anorexia in fish suffering enteromyxosis (Sitjà-Bobadilla and Palenzuela, 2012) are induced early in the infection. The down-regulation of other genes acting in the digestive process, although not numerous, also points towards diminished feeding activity and, in this sense, the up-regulation of *GCG2* may reflect the effort in maintaining euglycemia. Finally, *VIP* product also has been recognized as an immunomodulatory peptide with immunosuppressive function (Delgado et al., 2004), so its reduced

422 expression may be due to the immune defence response, as previously suggested (Bermúdez et al.,
423 2007).

424

425 *3.9. Conclusions*

426 The pathogenesis of enteromyxosis still has many unknown features, especially those related
427 to the incipient phase of infection. The parasite in the pre-patent period circumvents the host
428 response and successfully reaches and penetrates the intestinal lining epithelium. The findings of
429 this work constitute a basis for deciphering the mechanisms acting during this phase. A schematic
430 diagram summarizing the main results is presented in Fig. 6. The turbot immune response during
431 early enteromyxosis is chiefly characterized by signalling pathways involving IFNs, in contrast to
432 that observed in advanced infection, and only some mechanisms of innate immunity are shared
433 between both stages. There is some evidence of possible targets for parasite immune system evasion
434 such as complement components and APP, which possibly hinder a proper acute phase response. At
435 an intestinal level, the invasion and colonization strategies of *E. scophthalmi* appear to involve
436 cytoskeleton remodelling of the host cells and inhibition of epithelial renewal. Also, it is noteworthy
437 that one of the fish analyzed, which presented more mature and spreading stages of the myxozoan,
438 showed less intense transcriptomic changes. Further studies using more individuals or families are
439 required to ascertain the consistency and causes of this observation, although it suggests a silencing
440 of the host response, which would allow the early proliferation and colonization of vast areas of the
441 gastrointestinal lining epithelium by *E. scophthalmi*. Likely, when the parasite load and the related
442 tissue damage become important, the immune response is triggered. However, as pointed out by
443 different studies, this delayed response, which is exacerbated at a local level contributing to the
444 severe intestinal lesions, is ineffective. The transcriptomic analysis performed here has brought
445 novel and intriguing information about host-parasite interactions in enteromyxosis. The

identification of the molecular actors and their roles may speed the development of early detection, control and therapeutic strategies, and even to identify targets for breeding programs.

Acknowledgements

The authors would like to thank María José Redondo and María E. Alonso-Naveiro for the assistance with the infection trial. Also, we want to acknowledge Lucía Insua, María del Carmen Carreira and Sandra Maceiras for technical assistance. This study was funded by the Spanish Ministry of Economy and Competitiveness (AGL 2009-13282-C02-01 and -02; AGL2015-67039-C3-1-R and AGL2015-67039-C3-3-R), the European Regional Development's funds (FEDER) and Xunta de Galicia (Spain) local government (GRC2014/010 and GPC2015/34). Diego Robledo was supported by a FPU fellowship funded by the Spanish Ministry of Education, Culture and Sport. Paolo Ronza was supported by a grant from the scientific network "INMUNOGENOM", funded by Xunta de Galicia (REDES GI-1251). We acknowledge the support of the Centro de Supercomputación de Galicia (CESGA), Spain, in the completion of this work.

References

Armstrong, P.B., 2006. Proteases and protease inhibitors: a balance of activities in host-pathogen interaction. Immunobiology 211, 263-281.

APROMAR, 2015. La Acuicultura en España 2015. Available online at http://www.apromar.es/content/informes-anuales

Bayne, C.J., Gerwick, L., 2001. The acute phase response and innate immunity of fish. Dev Comp Immunol 25, 725-743.

Beiting, D.P., 2014. Protozoan parasites and type I interferons: a cold case reopened. Trends Parasitol 30, 491-498.

Ben-Othman, R., Flannery, A.R., Miguel, D.C., Ward, D.M., Kaplan, J., Andrews, N.W., 2014. *Leishmania*-mediated inhibition of iron export promotes parasite replication in macrophages. PLoS Pathog 10, e1003901.

Bermúdez, R., Losada, A.P., Vázquez, S., Redondo, M.J., Álvarez-Pellitero, P., Quiroga, M.I., 2010. Light and electron microscopic studies on turbot *Psetta maxima* infected with *Enteromyxum scophthalmi*: histopathology of turbot enteromyxosis. Dis Aquat Organ 89, 209-221.

Bermúdez, R., Vigliano, F., Marcaccini, A., Sitjà-Bobadilla, A., Quiroga, M.I., Nieto, J.M., 2006. Response of Ig-positive cells to *Enteromyxum scophthalmi* (Myxozoa) experimental infection in turbot, *Scophthalmus maximus* (L.): A histopathological and immunohistochemical study. Fish Shellfish Immunol 21, 501-512.

Bermúdez, R., Vigliano, F., Quiroga, M.I., Nieto, J.M., Bosi, G., Domeneghini, C., 2007. Immunohistochemical study on the neuroendocrine system of the digestive tract of turbot, *Scophthalmus maximus* (L.), infected by *Enteromyxum scophthalmi* (Myxozoa). Fish Shellfish Immunol 22, 252-263.

485 Bimal, S., Singh, S.K., Sinha, S., Pandey, K., Sinha, P.K., Ranjan, A., Bhattacharya, S.K., Das, P.,
486 2008. *Leishmania donovani*: role of CD2 on CD4+ T-cell function in Visceral
487 Leishmaniasis. Exp Parasitol 118, 238-246.

488 Bjork, S.J., Zhang, Y.A., Hurst, C.N., Alonso-Naveiro, M.E., Alexander, J.D., Sunyer, J.O.,
489 Bartholomew, J.L., 2014. Defenses of susceptible and resistant Chinook salmon
490 (*Oncorhynchus tshawytscha*) against the myxozoan parasite *Ceratomyxa shasta*. Fish
491 Shellfish Immunol 37, 87-95.

492 Bolger, A.M., Lohse, M., Usadel, B., 2014. Trimmomatic: a flexible trimmer for Illumina sequence
493 data. Bioinformatics 30, 2114-2120.

494 Castanier, C., Garcin, D., Vazquez, A., Arnoult, D., 2010. Mitochondrial dynamics regulate the
495 RIG-I-like receptor antiviral pathway. EMBO Rep 11, 133-138.

496 Cliffe, L.J., Humphreys, N.E., Lane, T.E., Potten, C.S., Booth, C., Grencis, R.K., 2005. Accelerated
497 intestinal epithelial cell turnover: a new mechanism of parasite expulsion. Science 308,
498 1463-1465.

499 Conesa, A., Gotz, S., Garcia-Gomez, J.M., Terol, J., Talon, M., Robles, M., 2005. Blast2GO: a
500 universal tool for annotation, visualization and analysis in functional genomics research.
501 Bioinformatics 21, 3674-3676.

502 Cortes, A., Munoz-Antoli, C., Martin-Grau, C., Esteban, J.G., Grencis, R.K., Toledo, R., 2015.
503 Differential alterations in the small intestine epithelial cell turnover during acute and chronic
504 infection with *Echinostoma caproni* (Trematoda). Parasit Vectors 8, 334.

505 Costa, V., Aprile, M., Esposito, R., Ciccodicola, A., 2013. RNA-Seq and human complex diseases:
506 recent accomplishments and future perspectives. Eur J Hum Genet 21, 134-142.

507 Chen, X.M., Huang, B.Q., Splinter, P.L., Orth, J.D., Billadeau, D.D., McNiven, M.A., LaRusso,
508 N.F., 2004. Cdc42 and the actin-related protein/neural Wiskott-Aldrich syndrome protein

509 network mediate cellular invasion by *Cryptosporidium parvum*. Infect Immun 72, 3011-
510 3021.

511 Davey, G.C., Calduch-Giner, J.A., Houeix, B., Talbot, A., Sitjà-Bobadilla, A., Prunet, P., Pérez-
512 Sánchez, J., Cairns, M.T., 2011. Molecular profiling of the gilthead sea bream (*Sparus*
513 *aurata* L.) response to chronic exposure to the myxosporean parasite *Enteromyxum leei*. Mol
514 Immunol 48, 2102-2112.

515 Delgado, M., Pozo, D., Ganea, D., 2004. The significance of vasoactive intestinal peptide in
516 immunomodulation. Pharmacol Rev 56, 249-290.

517 Dixit, E., Kagan, J.C., 2013. Intracellular pathogen detection by RIG-I-like receptors. Adv Immunol
518 117, 99-125.

519 Estensoro, I., Redondo, M.J., Álvarez-Pellitero, P., Sitjà-Bobadilla, A., 2014. Immunohistochemical
520 characterization of polyclonal antibodies against *Enteromyxum leei* and *Enteromyxum*
521 *scophthalmi* (Myxozoa: Myxosporea), intestinal parasites of fish. J Fish Dis 37, 785-796.

522 Figueras, A., Robledo, D., Corvelo, A., Hermida, M., Pereiro, P., Rubiolo, J.A., Gómez-Garrido, J.,
523 Carreté L., Bello, X., Gut, M., Gut, I.G., Marcet-Houben, M., Forn-Cuní, G., Abal-Fabeiro,
524 J.L., Pardo, B.G., Taboada, X., Fernández, C., Vlasova, A., Hermoso-Pulido, A., Guigó, R.,
525 Álvarez-Dios, J.A., Gómez-Tato, A., Viñas, A., Maside, X., Gabaldón, T., Novoa, B.,
526 Bouza, C., Alioto, T., Martínez, P., 2016. Whole genome sequencing of turbot
527 (*Scophthalmus maximus*; Pleuronectiformes): a fish adapted to demersal life. DNA Res, in
528 press, doi: 10.1093/dnares/dsw007.

529 Gerwick, L., Steinhauer, R., Lapatra, S., Sandell, T., Ortuno, J., Hajiseyedjavadi, N., Bayne, C.J.,
530 2002. The acute phase response of rainbow trout (*Oncorhynchus mykiss*) plasma proteins to
531 viral, bacterial and fungal inflammatory agents. Fish Shellfish Immunol 12, 229-242.

Gruenheid, S., Finlay, B.B., 2003. Microbial pathogenesis and cytoskeletal function. Nature 422, 775-781.

Iwai, H., Kim, M., Yoshikawa, Y., Ashida, H., Ogawa, M., Fujita, Y., Muller, D., Kirikae, T., Jackson, P.K., Kotani, S., Sasakawa, C., 2007. A bacterial effector targets Mad2L2, an APC inhibitor, to modulate host cell cycling. Cell 130, 611-623.

Kanehisa, M., Sato, Y., Kawashima, M., Furumichi, M., Tanabe, M., 2016. KEGG as a reference resource for gene and protein annotation. Nucleic Acids Res 44, D457-462.

Kashiwada, M., Cassel, S.L., Colgan, J.D., Rothman, P.B., 2011. NFIL3/E4BP4 controls type 2 T helper cell cytokine expression. EMBO J 30, 2071-2082.

Kautz, L., Jung, G., Valore, E.V., Rivella, S., Nemeth, E., Ganz, T., 2014. Identification of erythroferrone as an erythroid regulator of iron metabolism. Nat Genet 46, 678-684.

Khoo, C.-K., Abdul-Murad, A.M., Kua, B.-C., Mohd-Adnan, A., 2012. *Cryptocaryon irritans* infection induces the acute phase response in *Lates calcarifer*: A transcriptomic perspective. Fish Shellfish Immunol 33, 788-794.

Kim, D., Pertea, G., Trapnell, C., Pimentel, H., Kelley, R., Salzberg, S.L., 2013. TopHat2: accurate alignment of transcriptomes in the presence of insertions, deletions and gene fusions. Genome Biol 14, R36.

Kim, M., Ogawa, M., Mimuro, H., Sasakawa, C., 2010. Reinforcement of epithelial cell adhesion to basement membrane by a bacterial pathogen as a new infectious stratagem. Virulence 1, 52-55.

Kim, Y.E., Ahn, J.H., 2015. Positive role of promyelocytic leukemia protein in type I interferon response and its regulation by human cytomegalovirus. PLoS Pathog 11, e1004785.

Koshiba, T., 2013. Mitochondrial-mediated antiviral immunity. Biochim Biophys Acta 1833, 225-232.

Kovacevic, N., Hagen, M.O., Xie, J., Belosevic, M., 2015. The analysis of the acute phase response during the course of *Trypanosoma carassii* infection in the goldfish (*Carassius auratus* L.). Dev Comp Immunol 53, 112-122.

Langmead, B., Salzberg, S.L., 2012. Fast gapped-read alignment with Bowtie 2. Nat Methods 9, 357-359.

Leon-Sicairos, N., Reyes-Cortes, R., Guadrón-Llanos, A.M., Madueña-Molina, J., Leon-Sicairos, C., Canizalez-Román, A., 2015. Strategies of intracellular pathogens for obtaining iron from the environment. Biomed Res Int 2015, 17.

Li, C., Beck, B., Su, B., Terhune, J., Peatman, E., 2013. Early mucosal responses in blue catfish (*Ictalurus furcatus*) skin to *Aeromonas hydrophila* infection. Fish Shellfish Immunol 34, 920-928.

Li, C., Zhang, Y., Wang, R., Lu, J., Nandi, S., Mohanty, S., Terhune, J., Liu, Z., Peatman, E., 2012. RNA-seq analysis of mucosal immune responses reveals signatures of intestinal barrier disruption and pathogen entry following *Edwardsiella ictaluri* infection in channel catfish, *Ictalurus punctatus*. Fish Shellfish Immunol 32, 816-827.

Li, B., Dewey, C.N., 2011. RSEM: accurate transcript quantification from RNA-seq data with or without a reference genome. BMC Bioinformatics 12, 323.

Li, Q., Freeman, L.M., Rush, J.E., Huggins, G.S., Kennedy, A.D., Labuda, J.A., Laflamme, D.P., Hannah, S.S., 2015. Veterinary medicine and multi-omics research for future nutrition targets: metabolomics and transcriptomics of the common degenerative mitral valve disease in dogs. OMICS 19, 461-470.

Liu, J., Deng, M., Lancto, C.A., Abrahamsen, M.S., Rutherford, M.S., Enomoto, S., 2009. Biphasic modulation of apoptotic pathways in *Cryptosporidium parvum*-infected human intestinal epithelial cells. Infect Immun 77, 837-849.

Lodge, R., Descoteaux, A., 2006. Phagocytosis of *Leishmania donovani* amastigotes is Rac1 dependent and occurs in the absence of NADPH oxidase activation. Eur J Immunol 36, 2735-2744.

Losada, A.P., Bermúdez, R., Faílde, L.D., de Ocenda, M.V.R., Quiroga, M.I., 2014a. Study of the distribution of active caspase-3-positive cells in turbot, *Scophthalmus maximus* (L.), enteromyxosis. J Fish Dis 37, 21-32.

Losada, A.P., Bermúdez, R., Faílde, L.D., Di Giancamillo, A., Domeneghini, C., Quiroga, M.I., 2014b. Effects of *Enteromyxum scophthalmi* experimental infection on the neuroendocrine system of turbot, *Scophthalmus maximus* (L.). Fish Shellfish Immunol 40, 577-583.

Losada, A.P., Bermúdez, R., Faílde, L.D., Quiroga, M.I., 2012. Quantitative and qualitative evaluation of iNOS expression in turbot (*Psetta maxima*) infected with *Enteromyxum scophthalmi*. Fish Shellfish Immunol 32, 243-248.

Luo, M., Sainsbury, J., Tuff, J., Lacap, P.A., Yuan, X.Y., Hirbod, T., Kimani, J., Wachihi, C., Ramdahin, S., Bielawny, T., Embree, J., Broliden, K., Ball, T.B., Plummer, F.A., 2012. A genetic polymorphism of FREM1 is associated with resistance against HIV infection in the Pumwani sex worker cohort. J Virol 86, 11899-11905.

Manocha, G.D., Mishra, R., Sharma, N., Kumawat, K.L., Basu, A., Singh, S.K., 2014. Regulatory role of TRIM21 in the type-I interferon pathway in Japanese encephalitis virus-infected human microglial cells. J Neuroinflammation 11, 24.

McEwan, W.A., Tam, J.C.H., Watkinson, R.E., Bidgood, S.R., Mallery, D.L., James, L.C., 2013. Intracellular antibody-bound pathogens stimulate immune signaling via the Fc receptor TRIM21. Nat Immunol 14, 327-336.

McGavin, D., Zachary, J.F., 2006. Pathologic Basis of Veterinary Disease. Elsevier Health Sciences, New York, NY, USA.

Melo, M.B., Nguyen, Q.P., Cordeiro, C., Hassan, M.A., Yang, N., McKell, R., Rosowski, E.E., Julien, L., Butty, V., Darde, M.L., Ajzenberg, D., Fitzgerald, K., Young, L.H., Saeij, J.P., 2013. Transcriptional analysis of murine macrophages infected with different *Toxoplasma* strains identifies novel regulation of host signaling pathways. PLoS Pathog 9, e1003779.

Mimuro, H., Suzuki, T., Nagai, S., Rieder, G., Suzuki, M., Nagai, T., Fujita, Y., Nagamatsu, K., Ishijima, N., Koyasu, S., Haas, R., Sasakawa, C., 2007. *Helicobacter pylori* dampens gut epithelial self-renewal by inhibiting apoptosis, a bacterial strategy to enhance colonization of the stomach. Cell Host Microbe 2, 250-263.

Mittal, K., Welter, B.H., Temesvari, L.A., 2008. *Entamoeba histolytica*: lipid rafts are involved in adhesion of trophozoites to host extracellular matrix components. Exp Parasitol 120, 127-134.

Moon, T.W., 1998. Glucagon: from hepatic binding to metabolism in teleost fish. Comp Biochem Phys B 121, 27-34.

Nde, P.N., Lima, M.F., Johnson, C.A., Pratap, S., Villalta, F., 2012. Regulation and use of the extracellular matrix by *Trypanosoma cruzi* during early infection. Front Immunol 3, 337.

Nie, L., Xiong, R., Zhang, Y.S., Zhu, L.Y., Shao, J.Z., Xiang, L.X., 2014. Conserved inhibitory role of teleost SOCS-1s in IFN signaling pathways. Dev Comp Immunol 43, 23-29.

Onoguchi, K., Onomoto, K., Takamatsu, S., Jogi, M., Takemura, A., Morimoto, S., Julkunen, I., Namiki, H., Yoneyama, M., Fujita, T., 2010. Virus-infection or 5'ppp-RNA activates antiviral signal through redistribution of IPS-1 mediated by MFN1. PLoS Pathog 6, e1001012.

Peatman, E., Baoprasertkul, P., Terhune, J., Xu, P., Nandi, S., Kucuktas, H., Li, P., Wang, S., Somridhivej, B., Dunham, R., Liu, Z., 2007. Expression analysis of the acute phase response

in channel catfish (*Ictalurus punctatus*) after infection with a Gram-negative bacterium. Dev Comp Immunol 31, 1183-1196.

Pereiro, P., Figueras, A., Novoa, B., 2012. A novel hepcidin-like in turbot (*Scophthalmus maximus* L.) highly expressed after pathogen challenge but not after iron overload. Fish Shellfish Immunol 32, 879-889.

Peterson, L.W., Artis, D., 2014. Intestinal epithelial cells: regulators of barrier function and immune homeostasis. Nat Rev Immunol 14, 141-153.

Qian, X., Ba, Y., Zhuang, Q., Zhong, G., 2014. RNA-Seq technology and its application in fish transcriptomics. OMICS 18, 98-110.

Quiroga, M.I., Redondo, M.J., Sitjà-Bobadilla, A., Palenzuela, O., Riaza, A., Macías, A., Vázquez, S., Pérez, A., Nieto, J.M., Álvarez-Pellitero, P., 2006. Risk factors associated with *Enteromyxum scophthalmi* (Myxozoa) infection in cultured turbot, *Scophthalmus maximus* (L.). Parasitology 133, 433-442.

Radhakrishnan, G.K., Splitter, G.A., 2012. Modulation of host microtubule dynamics by pathogenic bacteria. Biomol Concepts 3, 571-580.

Redondo, M.J., Álvarez-Pellitero, P., 2010. The effect of lectins on the attachment and invasion of *Enteromyxum scophthalmi* (Myxozoa) in turbot (*Psetta maxima* L.) intestinal epithelium in vitro. Exp Parasitol 126, 577-581.

Redondo, M.J., Palenzuela, O., Álvarez-Pellitero, P., 2004. Studies on transmission and life cycle of *Enteromyxum scophthalmi* (Myxozoa), an enteric parasite of turbot *Scophthalmus maximus*. Folia Parasitol (Praha) 51, 188-198.

Redondo, M.J., Palenzuela, O., Riaza, A., Macías, A., Álvarez-Pellitero, P., 2002. Experimental transmission of *Enteromyxum scophthalmi* (Myxozoa), an enteric parasite of turbot *Scophthalmus maximus*. J Parasitol 88, 482-488.

Redondo, M.J., Quiroga, M.I., Palenzuela, O., Nieto, J.M., Álvarez-Pellitero, P., 2003. Ultrastructural studies on the development of *Enteromyxum scophthalmi* (Myxozoa), an enteric parasite of turbot (*Scophthalmus maximus* L.). Parasitol Res 90, 192-202.

Robinson, M.D., Oshlack, A., 2010. A scaling normalization method for differential expression analysis of RNA-seq data. Genome Biol 11, R25.

Robledo, D., Ronza, P., Harrison, P.W., Losada, A.P., Bermúdez, R., Pardo, B.G., Redondo, M.J., Sitjà-Bobadilla, A., Quiroga, M.I., Martínez, P., 2014. RNA-seq analysis reveals significant transcriptome changes in turbot (*Scophthalmus maximus*) suffering severe enteromyxosis. BMC Genomics 15, 1149.

Simpson, J.T., Wong, K., Jackman, S.D., Schein, J.E., Jones, S.J.M., Birol, I., 2009. ABySS: A parallel assembler for short read sequence data. Genome Res 19, 1117-1123.

Singh, B., Fleury, C., Jalalvand, F., Riesbeck, K., 2012. Human pathogens utilize host extracellular matrix proteins laminin and collagen for adhesion and invasion of the host. FEMS Microbiol Rev 36, 1122-1180.

Sitjà-Bobadilla, A., Palenzuela, O., 2012. *Enteromyxum* Species, in: Woo, P.T.K., Buchmann, K. (Eds.), Fish Parasites: Pathobiology and Protection. CABI publishing, UK, pp. 163-176.

Sitjà-Bobadilla, A., Redondo, M.J., Bermúdez, R., Palenzuela, O., Ferreiro, I., Riaza, A., Quiroga, I., Nieto, J.M., Álvarez-Pellitero, P., 2006. Innate and adaptive immune responses of turbot, *Scophthalmus maximus* (L.), following experimental infection with *Enteromyxum scophthalmi* (Myxosporea: Myxozoa). Fish Shellfish Immunol 21, 485-500.

Sun, F., Peatman, E., Li, C., Liu, S., Jiang, Y., Zhou, Z., Liu, Z., 2012. Transcriptomic signatures of attachment, NF-kappaB suppression and IFN stimulation in the catfish gill following columnaris bacterial infection. Dev Comp Immunol 38, 169-180.

674 Suzuki, T., 2013. Regulation of intestinal epithelial permeability by tight junctions. Cell Mol Life
675 Sci 70, 631-659.

676 Tran, D.Q., Andersson, J., Wang, R., Ramsey, H., Unutmaz, D., Shevach, E.M., 2009. GARP
677 (LRRC32) is essential for the surface expression of latent TGF-beta on platelets and
678 activated FOXP3+ regulatory T cells. Proc Natl Acad Sci U S A 106, 13445-13450.

679 Vaysburd, M., Watkinson, R.E., Cooper, H., Reed, M., O'Connell, K., Smith, J., Cruickshanks, J.,
680 James, L.C., 2013. Intracellular antibody receptor TRIM21 prevents fatal viral infection.
681 Proc Natl Acad Sci U S A 110, 12397-12401.

682 Wu, J., Mao, X., Cai, T., Luo, J., Wei, L., 2006. KOBAS server: a web-based platform for
683 automated annotation and pathway identification. Nucleic Acids Res 34, W720-W724.

684 Xu, J.H., Qin, Z.H., Liao, Y.S., Xie, M.Q., Li, A.X., Cai, J.P., 2008. Characterization and
685 expression of an actin-depolymerizing factor from *Eimeria tenella*. Parasitol Res 103, 263-
686 270.

687 Young, N.D., Cooper, G.A., Nowak, B.F., Koop, B.F., Morrison, R.N., 2008. Coordinated down-
688 regulation of the antigen processing machinery in the gills of amoebic gill disease-affected
689 Atlantic salmon (*Salmo salar* L.). Mol Immunol 45, 2581-2597.

690 Zhang, J., Yu, L.P., Li, M.F., Sun, L., 2014. Turbot (*Scophthalmus maximus*) hepcidin-1 and
691 hepcidin-2 possess antimicrobial activity and promote resistance against bacterial and viral
692 infection. Fish Shellfish Immunol 38, 127-134.

693 Zhang, W., Zhang, J., Kornuc, M., Kwan, K., Frank, R., Nimer, S.D., 1995. Molecular cloning and
694 characterization of NF-IL3A, a transcriptional activator of the human interleukin-3
695 promoter. Mol Cell Biol 15, 6055-6063.

Zhou, Y., Liang, X.-F., Yuan, X., Li, J., He, Y., Fang, L., Guo, X., Liu, L., Li, B., Shen, D., 2013. Neuropeptide Y stimulates food intake and regulates metabolism in grass carp, *Ctenopharyngodon idellus*. Aquaculture 380–383, 52-61.

Zipfel, P.F., Wurzner, R., Skerka, C., 2007. Complement evasion of pathogens: common strategies are shared by diverse organisms. Mol Immunol 44, 3850-3857.

Zou, J., Secombes, C.J., 2011. Teleost fish interferons and their role in immunity. Dev Comp Immunol 35, 1376-1387.

TABLES

Table 1. Comparison between genome-guided and de novo transcriptome assemblies from RNA-seq data obtained from samples of control and *Enteromyxum scophthalmi*-infected turbot (*Scophthalmus maximus*).

	Genome-guided	**De novo**
Number of reads	160 million	-
Reads mapped to the genome	138 million	-
Reads for de novo assembly	-	18 million[a]
Total transcripts	56,321	328,480
N50 [b]	5073	1510

[a] Total unaligned reads from pyloric caeca samples at 24 and 42 days post-inoculation.

[b]N50 is the length for which the collection of all transcripts of that length or longer contains at least half of the sum of the lengths of all transcripts.

FIGURE LEGENDS

Fig. 1. Histopathology (A, B, D, E; stained with toluidine blue) and immunohistochemistry (C, F) of pyloric caeca from turbot (*Scophthalmus maximus*) infected by *Enteromyxum scophthalmi*. (A) Note the slight inflammatory infiltration at the basal part of the lining epithelium (arrowhead) and in the lamina propria-submucosa (asterisk). Also, round basophilic structures can be seen in the epithelial lining of an intestinal fold (black arrows). Scale bar = 100 μm. (B) Higher magnification of pyloric caeca showing the infiltration of mononuclear cells in the basal part of the epithelium (arrowhead) and the lamina propria-submucosa (black arrow). Note the round basophilic structures

718 near the basement membrane of the epithelial lining (white arrow), consistent with early
719 development stages of *E. scophthalmi*. Scale bar = 50 μm. (C) Immunohistochemical detection of
720 two early stages of *E. scophthalmi* (brown colored) in the basal part of the epithelium. Scale bar =
721 20 μm. (D - F) Histological section from the pyloric caeca of the infected turbot 2. (D) Note the
722 presence of two parasitic structures in the epithelial lining, associated with a very mild
723 inflammatory infiltration. Scale bar = 100 μm. (E) Higher magnification showing a trophozoite
724 (arrowhead), consistent with a developmental stage 3 of *E. scophthalmi*. Scale bar = 50 μm. (F)
725 Immunostaining of a parasitic structure with the polyclonal antibody against *E. scophthalmi*. Scale
726 bar = 20 μm.

727

728 **Fig. 2.** Hierarchical clustering of samples by organ from turbot (*Scophthalmus maximus*) at 24 days
729 post-inoculation with *Enteromyxum scophthalmi* . Hierarchical clustering of all infected (-1, -2, -3)
730 and control (Ctrl) samples for (A) head kidney, (B) spleen and (C) pyloric caeca. Approximate
731 unbiased *P* values, computed by multi-scale bootstrap resampling, are displayed on branch nodes.

732

733 **Fig. 3.** Heatmaps of differentially expressed genes of interest in turbot (*Scophthalmus maximus*) at
734 24 days post-inoculation with *Enteromyxum scophthalmi*. Heatmaps for (A) head kidney, (B) spleen
735 and (C) pyloric caeca showing the expression of several genes of interest, labelling their functional
736 category. Displayed are EdgeR (Robinson and Oshlack, 2010) normalized counts for each sample
737 and gene. Expression values for each gene have been scaled from -1 to 1 by subtracting the mean
738 and dividing by the standard deviation. Genes were hierarchically clustered according to their gene
739 expression using Pearson correlation as a distance measure. 1, 2, 3, infected turbot numbers 1, 2, 3;
740 C, control. Full names of genes are shown in Supplementary Tables S2 - S4.

741

742 **Fig. 4.** Gene Ontology (GO) term enrichment among the differentially expressed genes for (A) head
743 kidney, (B) spleen and (C) pyloric caeca from turbot (*Scophthalmus maximus*) at 24 days post-
744 inoculation with *Enteromyxum scophthalmi*.

745

746 **Fig. 5.** Venn diagrams showing differentially expressed genes in (A) head kidney, (B) spleen and
747 (C) pyloric caeca from slightly (24d) and severely (42d) infected turbot (*Scophthalmus maximus*),
748 corresponding to 24 and 42 days post-inoculation with *Enteromyxum scophthalmi*.

749

750 **Fig. 6.** Schematic diagram showing the main events involved in early enteromyxosis in turbot
751 (*Scophthalmus maximus*) inferred from the results of this study. ECM, extra-cellular matrix.

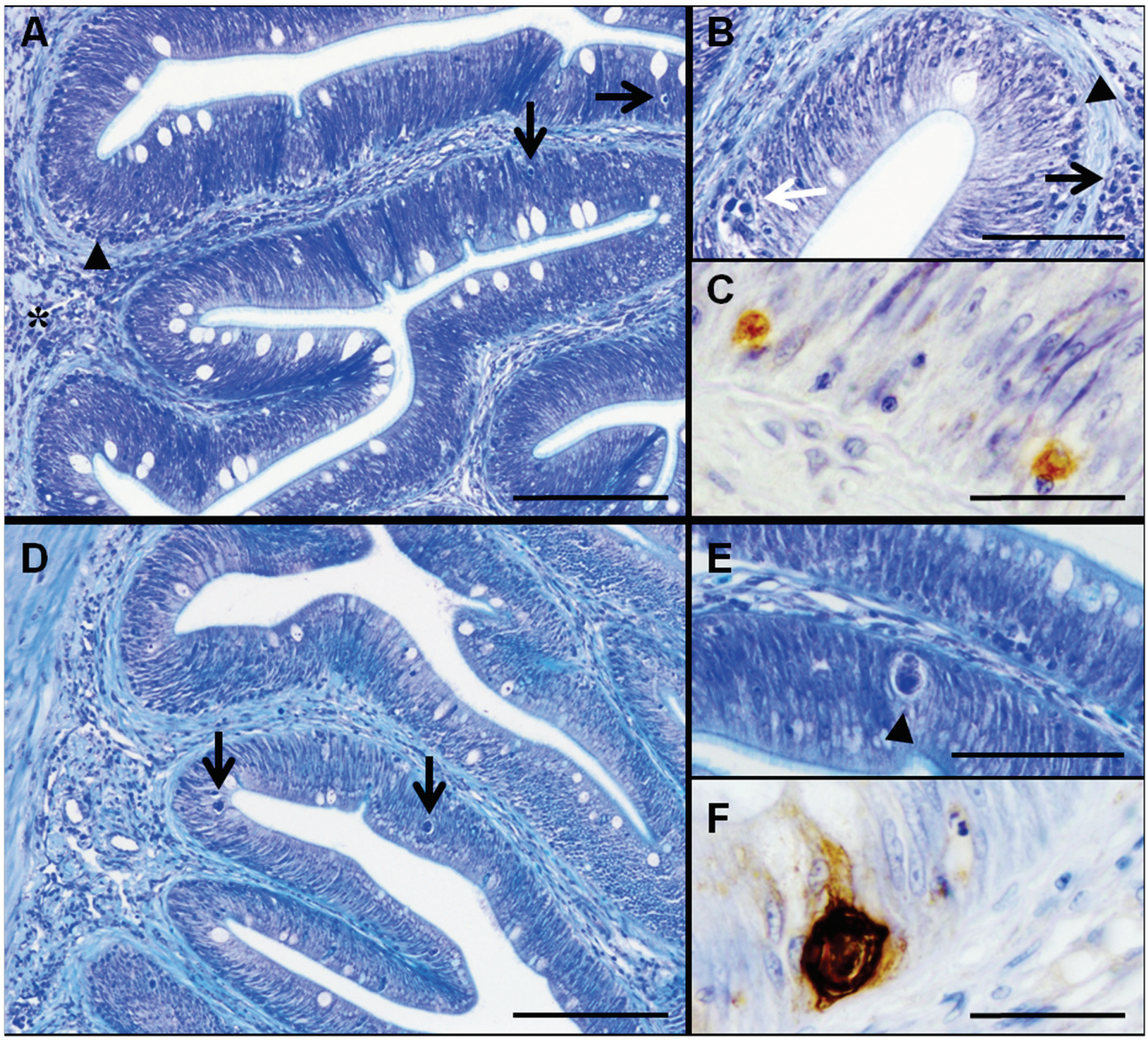

752

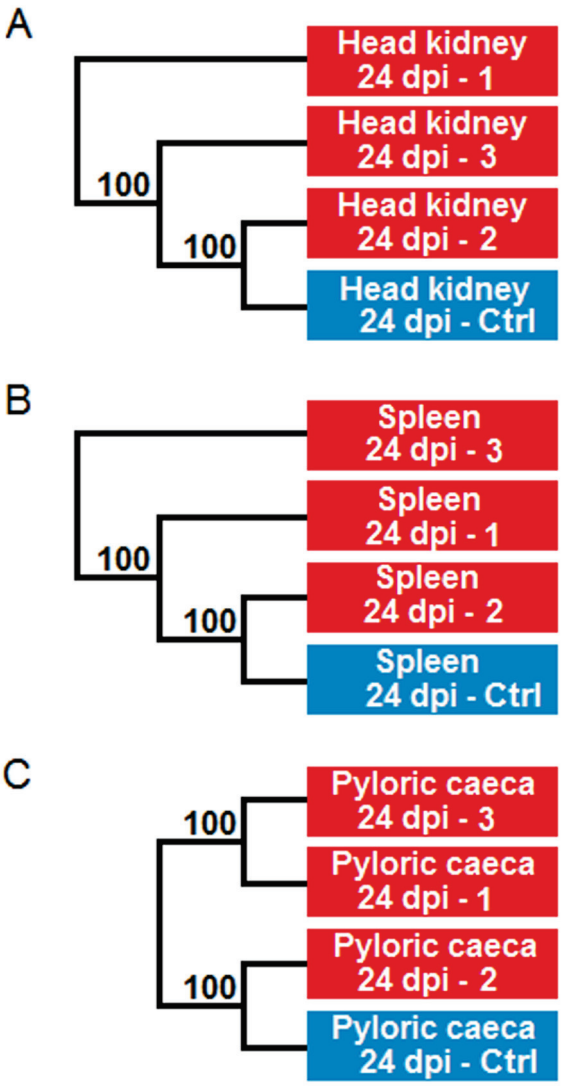

753

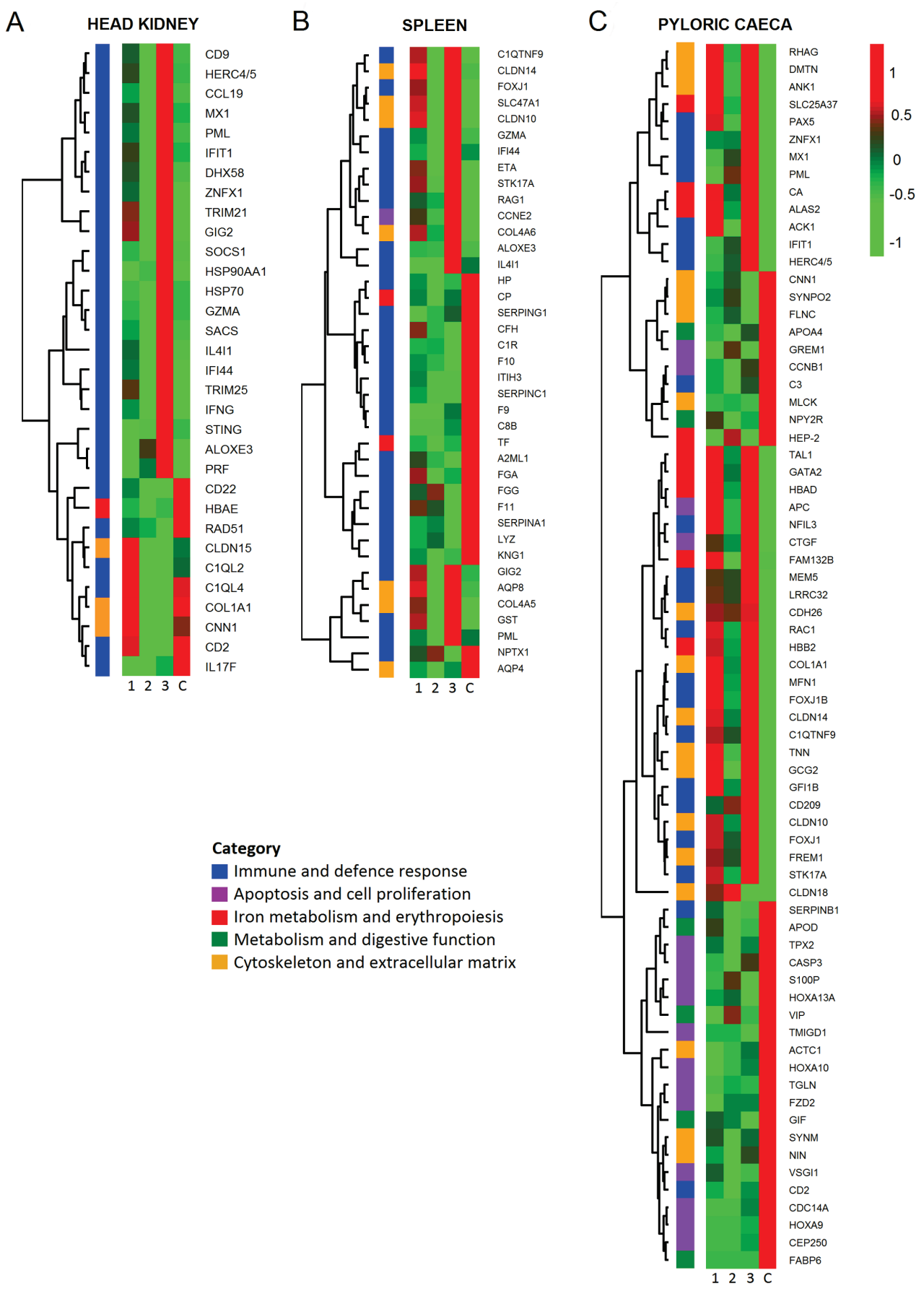

754

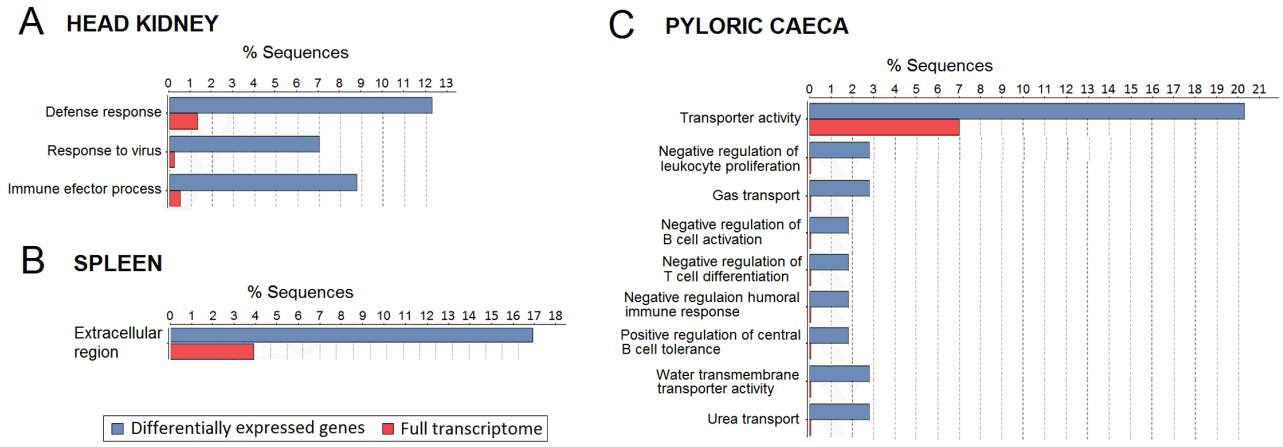

755

756

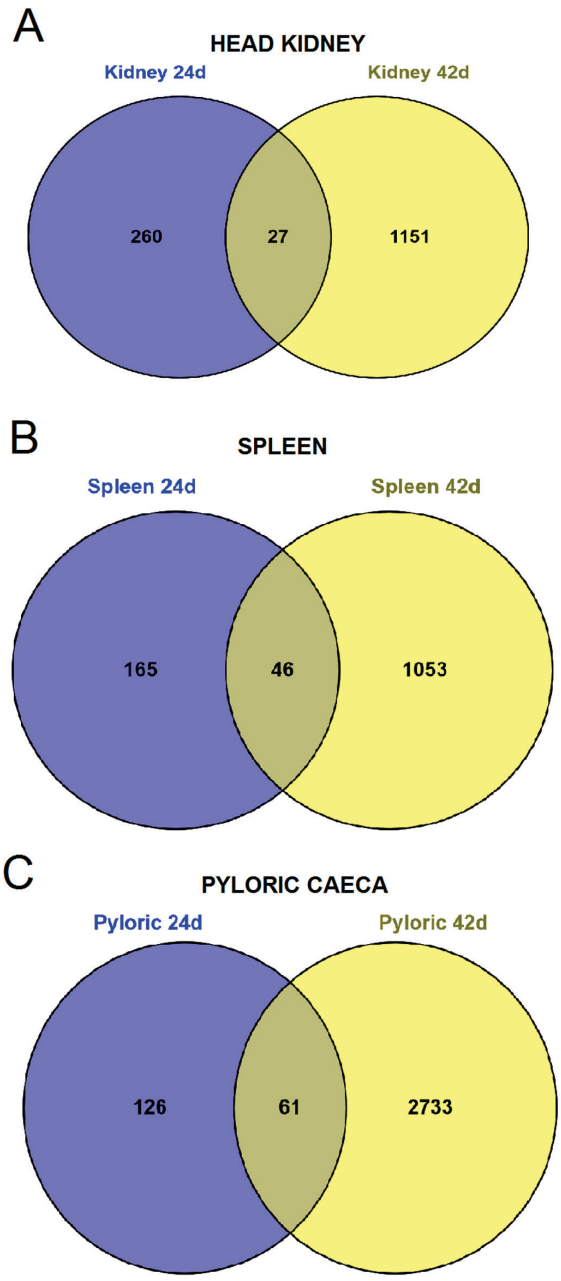

757

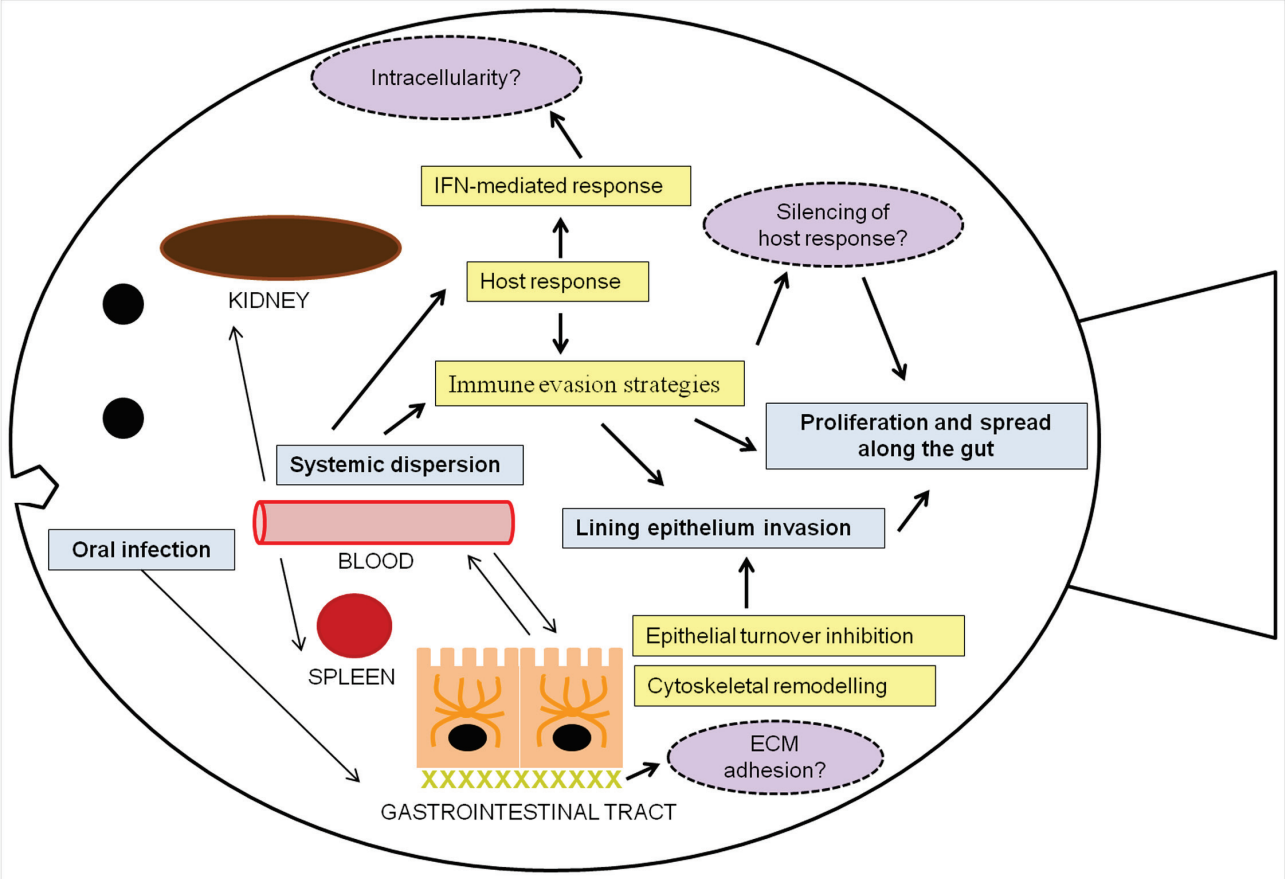

SUPPLEMENTARY FIGURE LEGEND

Supplementary Fig. S1. Illustration of the Kyoto Encyclopedia of Genes and Genomes (KEGG) pathway "complement and coagulation cascades", which was statistically enriched (false discovery rate (FDR) corrected *P* value < 0.05) among the differentially expressed (DE) genes in the spleen of *Enteromyxum scophthalmi*-infected turbot (*Scophthalmus maximus*). The genes belonging to this pathway that were DE in the spleen of infected turbot are highlighted in red.

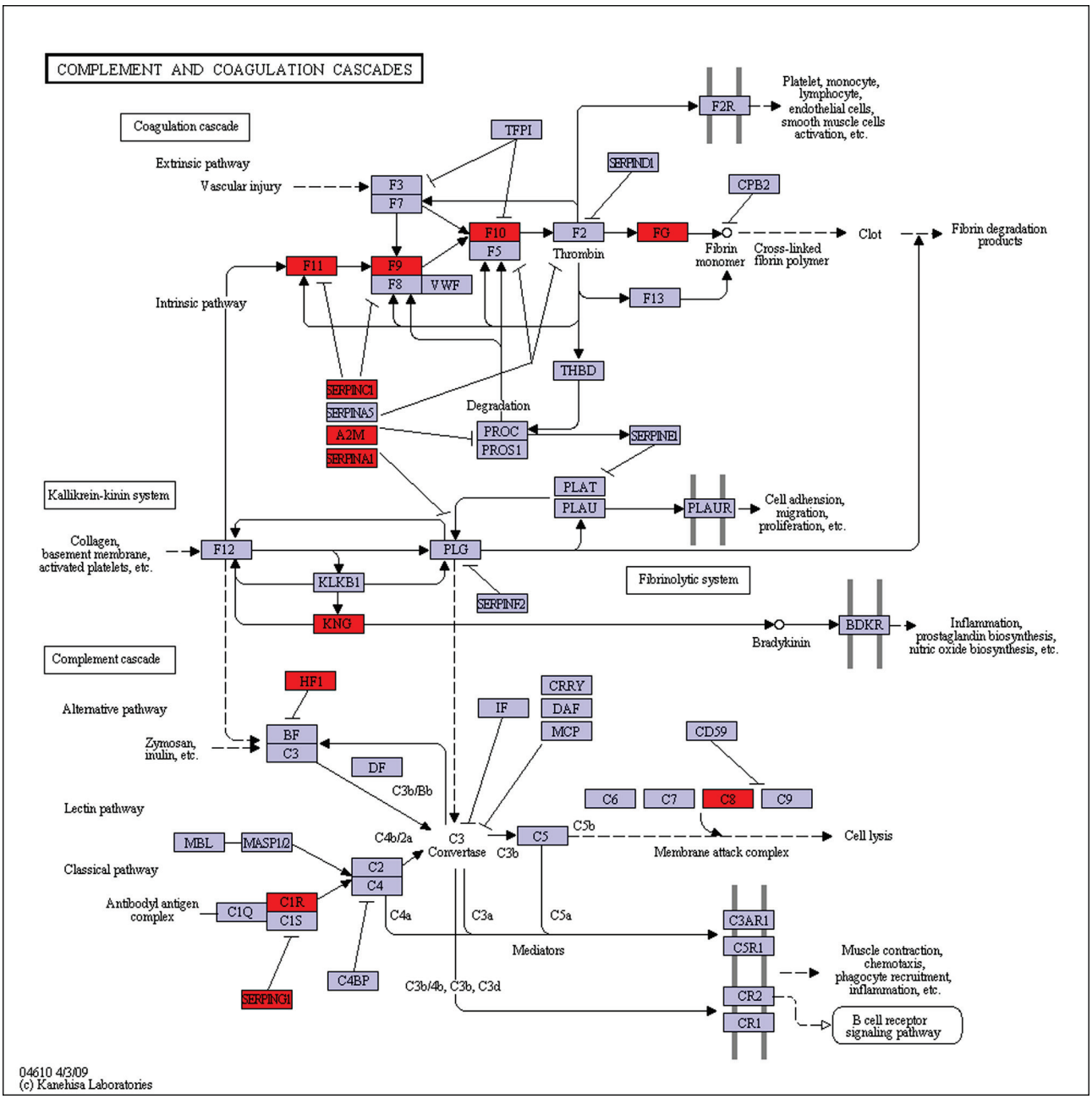

SUPPLEMENTARY TABLES

Supplementary tables S1 to S7 are available on the publisher Web site.

